Wetting Effects and Molecular Adsorption at Hydrated Kaolinite Clay Mineral Surfaces

Thomas Underwood, Valentina Erastova, and H. Chris Greenwell[*]

Department of Earth Sciences, Durham University, South Road, Durham DH1 3LE, U.K.

E-mail: chris.greenwell@durham.ac.uk

---
[*]To whom correspondence should be addressed

Abstract

In this study, classical molecular dynamics simulations have been used to understand the key interactions and surface structure of a set of organic molecules at the hydrated surfaces of the 1:1 clay mineral kaolinite. Decane, decanoic acid and decanamine have been modelled at both the hydroxylated and silicate surfaces of kaolinite. Additionally, the effect of pH is observed *via* looking at the protonated decanamine and decanoate anion forms. The key results show that relative affinity of the organic molecules to the kaolinite surface may be readily switched between the hydroxylated and silicate surfaces according to the pH and the nature of the organic head functional group. Decane molecules readily form droplets atop the silicate surface and do not adsorb to the hydroxyl surface, as do protonated decanoic acids. In stark contrast, decanoate anions do not adsorb to the silicate surface, yet adsorb to the hydroxyl surface through an anion exchange mechanism. Decanamine readily adsorbs to both silicate and hydroxyl surfaces, though the hydroxyl-amine interactions are mediated through water bridges. Once charged, the decanamine remains adsorbed to both surfaces, however, both interactions are ionically mediated, rather than through van der Waals and hydrogen bonds. Furthermore, protonated decanamine is observed to adsorb to the hydroxyl surface *via* anion bridges, a phenomenon that is typically associated with positively charged layered double hydroxides rather than negatively charged clay minerals.

2

1 Introduction

Hydrated mineral surfaces play an important role in many geochemical processes, whether within lacustrine/marine systems, terrestrial soils, aeolian dusts or within the subsurface in aquifers and oil reservoirs.[1] Under hydrous conditions, stable mineral surfaces include the silicates, carbonates, (oxy)hydroxides, *inter alia*.[2,3] Furthermore, a wide spectrum of low molecular weight organic molecules can exist within the natural environment, either as a result of natural processes or through anthropogenic inputs. Such organics encompass, amongst others, herbicides and pesticides, nutrients/fertilisers and detrital materials, weathered organic matter from peats and soils (typically humic and fulvic acids), crude oil derived hydrocarbons, fats/oils, explosives, pharmaceuticals, endocrine disrupting chemicals, etc. Owing to the moderate abundance of aqueous or humid environments, coupled with a relatively high hydration energy of many minerals, the interactions between minerals and organic molecules rarely involve ideal dry surfaces, but are far more likely to occur at hydrated surfaces with consequently very different physi- and chemisorption properties.[4]

Owing to the abundance of silica within the Earth's crust, weathering processes and hydrothermal alteration results in the formation of finegrained silicate minerals. When aluminum becomes incorporated in the structure, aluminosilicate minerals form, including the cation exchange mineral families: zeolites and clay minerals.[5] As a result of their high surface area and cation exchange properties, these minerals, whether from natural deposits or synthetic analogues, have found multiple practical applications and have been extensively studied using both analytical laboratory based techniques as well as molecular simulations.[6–8] The surfaces of both zeolite and clay minerals present an interesting contrast to silicate minerals as surface bound exposed cations possess a large enthalpy of hydration and (depending on the cation) present water wetting domains, where as the silicate domains behave more akin to quartz, with hydrophobic properties.[9]

Though the clay minerals with large cation exchange capacity are of significant interest, they constitute a far smaller fraction of total soil mineral content relative to the alumi-

nosilicate kaolinite minerals.[10] Kaolinite minerals make up a significant volume fraction of soil, aeolian and riverine/lacustrine minerals, and also a significant proportion of available surfaces in sandstone oil reservoirs.[11] Kaolinite is noted for its industrial applications, particularly in the production of porcelain and other ceramics, as a coating agent in, for example, paper production and also as an adsorbent and binder. These applications arise owing to the properties of kaolinite as a result of its structure.

1.1   Kaolinite Structure and Properties

Clay minerals, along with quartz, often form surface coatings in the pores of sandstone reservoirs,[5] as can be seen from scanning electron and atomic force microscopy for example, Figure 1. Illites, smectites, illite-smectites mixed layers and kaolinites are amongst the most abundant types of clay mineral found within sandstone reservoirs,[5] and whilst illites and smectites are generally considered as water-wetting, kaolinite is considered to be oil-wetting.[4]
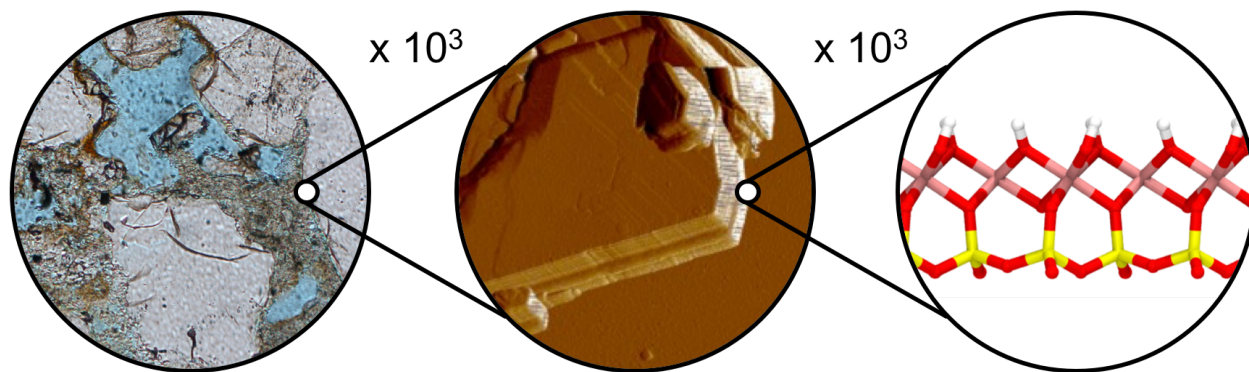

Figure 1: Electron scanning microscope image (left) of a sandstone core presenting a composition of large quartz grains (silver), pore water (blue) and clay minerals between quartz grains (grey and brown). Atomic force microscope image of kaolinite grains stacked upon each other (center), and the atomic structure of a single kaolinite layer (right).[12]

Structurally, kaolinite is a member of the 1:1 non-swelling group of clay minerals, where the structure of each layer is composed of one tetrahedral (T) SiO_4 sheet bonded to a gibbsite-

like octahedral (O) AlO_6 sheet, giving rise to an OT structure (Figure 1, right). The cation exchange clay minerals mainly belong to the 2:1 clay minerals, where the octahedral layer is sandwiched between two tetrahedral sheets (TOT repeat unit). As such, while the 2:1 clay minerals present a similar basal surface either side of the layer mid-plane, in kaolinite the upper and lower surfaces of one sheet are very different, where the gibbsite-like oxygens are often terminated by hydrogen atoms, creating a layer of hydroxyl groups. Henceforth, the gibbsite-like layer shall be referred to as the *hydroxyl surface*, whilst the SiO_4 layer shall be referred to as the *siloxane surface*.

Due to the low amount of isomorphic substitutions in kaolinite, kaolinite group clay minerals (including dickite and nacrite) do not have a permanent charge and do not swell, and the majority of clay-organic interactions occur either at particle basal planes or at at clay edge sites. In contrast, swelling 2:1 clays interact with organic matter at basal planes, edge sites and within the intercalated region between adjacent clay sheets.[1] The surface charge of kaolinite is pH dependent, as deprotonation of the hydroxyl groups can induce a net negative charge, however, in most instances, the major charge sites of kaolinite occur along the edges, rather than on the basal planes, of the clay particle.[13–15]

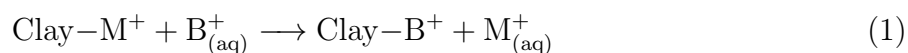## 1.2   Kaolinite-Organic Adsorption Mechanisms

The possible adsorption mechanisms of small organic molecules on clay basal surfaces have been previously studied in the literature.[16] Table 1 presents the important reported adsorption mechanisms between clay and organic molecules, and the relevant functional groups associated with each adsorption mechanism.

The exchange mechanisms in Table 1 (cation and anion exchange) describe the dynamic replacement of a small metal ion M initially adsorbed to a clay surface by a larger organic molecule, functional group B. The cation exchange mechanism, see Figure 2 (left), can be

Mechanism	Organic functional group
Cation exchange	Amino, ring NH, heterocyclic N (aromatic ring)
Anion exchange	Carboxylate
Water bridging	Amino, carboxylate, carbonyl, alcoholic OH
Cation bridging	Carboxylate, amines, carbonyl, alcoholic OH
Hydrogen bonding	Amino, carbonyl, carboxyl, phenolic OH
Van der Waals interaction	Uncharged organic units

represented by the formula:

$$\text{Clay}-\text{M}^+ + \text{B}^+_{(aq)} \longrightarrow \text{Clay}-\text{B}^+ + \text{M}^+_{(aq)} \tag{1}$$

In this instance, B usually refers to a organic molecule with a quaternary nitrogen atom (in this study -NH_3^+) and M is typically a monovalent cation (for example, Na^+).
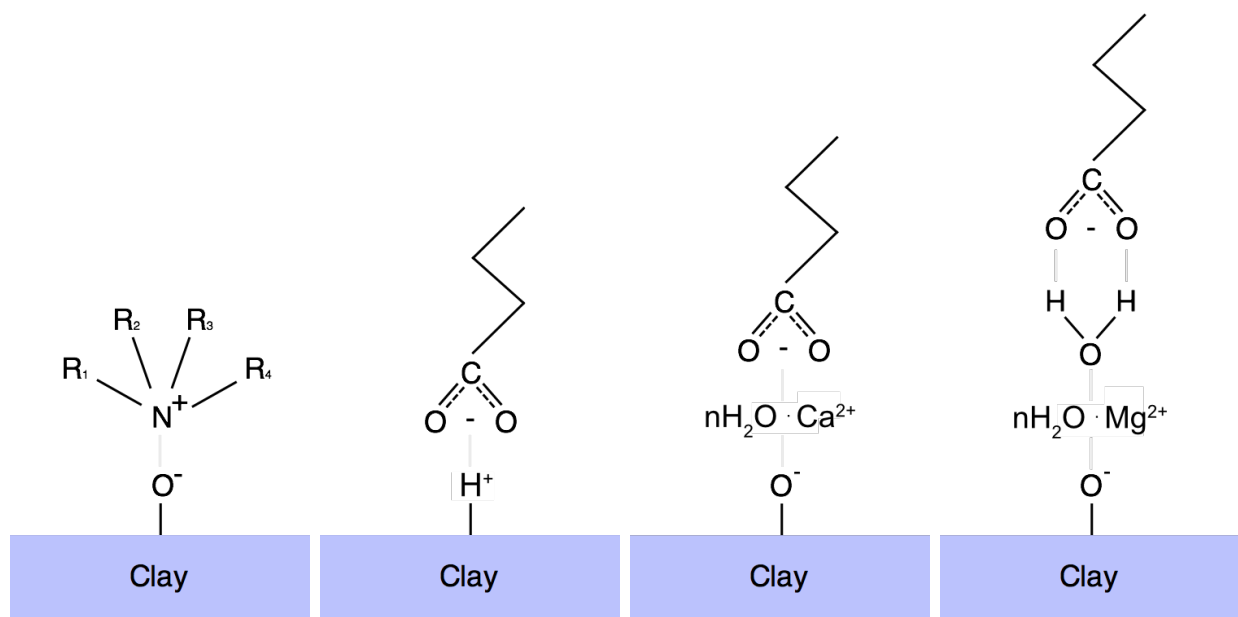

Figure 2: A schematic of four proposed organic-clay adsorption mechanisms. Left presents an example of cation exchange, where an organic molecule is directly bound to the clay. Center left presents the analogous mechanism, anion exchange. Center right presents cation bridging, whereby a hydrated divalent ion bridges a charged organic molecule to a like-charged clay surface. Right is an example of water bridging, whereby an organic molecule is adsorbed to the clay through several separate molecules including water.

Anion exchange is the analogous mechanism to cation exchange. In this case, the organic

molecule contains a negatively charged functional group, for example a carboxyl, and M is a univalent exchangeable anion bound to a protonated surface hydroxyl group or clay edge site. The mechanisms is thought to be more prominent in metal hydroxides (the positively charged clay counterpart) compared to negatively charged clay minerals.[16]

Cation and water bridging mechanisms, see Figure 2 (center right and right respectively), are both weak bonding mechanisms between clay and organic molecules. Water bridging can be represented by the formula:

$$\text{Clay}-\text{M}(\text{H}_2\text{O}) + \text{B}_{(aq)} \longrightarrow \text{Clay}-\text{M}(\text{H}_2\text{O})\text{B} \tag{2}$$
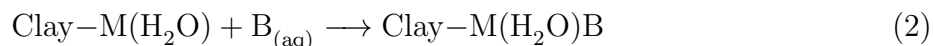
where B is an anionic or polar functional group and M is a hydrated exchangeable cation. Water bridging is thought to be more prevalent in the presence of strongly solvated cations (for example Mg^{2+}), since B is less likely to displace the bridging water molecule in such instances. When a direct bond is formed between B and M, the bonding mechanism is known as cation bridging.

Hydrogen bonding between organics and clay sites typically occur between -OH functional groups of an organic and mineral surface oxygens. The hydrogen bonding mechanism is proposed to be scarce and is weakly bonding as the clay surface oxygens are not excessively electronegative.[16] The van der Waals interaction mechanism, in contrast, occurs between all organics and a clay surface, and is ever-present.

1.3   Previous Simulation Studies of Kaolinite

Computational simulations offer great potential to examine the properties of clay mineral interfaces at an atomistic level. Previous simulation studies of clay mineral surfaces are widespread, and have broached a vast array of topics, from clay disordering, to dynamics and hydration. In particular, the use of computational simulations to study the properties of organic molecules at or on mineral surfaces has provided fertile ground for research (see

the article by Greenwell et al.[8] for a recent review on the uses of molecular simulations for clay minerals). Whilst mineral-organic interfaces have been heavily studied in the past, previous simulation studies of kaolinite minerals in particular, have primarily focused on the adsorption mechanisms of either a single molecule, or a relatively small number, of organic molecules to the clay surface.

Ab-initio quantum mechanical density functional theory (DFT) calculations have been used to model the adsorption of simple monomers,[17] sugars[18] and saturated hydrocarbons[19] on both the hydroxyl and the siloxane surfaces of kaolinite. Most studies observe a preference for organic adsorption to the hydrophilic hydroxyl surface, compared to the hydrophobic siloxane surface, due to the formation of short lived hydrogen bonds between the surface, the organic, and mediating water molecules.[17–19] With the inclusion of charged species and salts, ionic interactions become more favourable than the hydrogen bonds and become the primary cause of organic adsorption to the hydroxyl surface.[17] Furthermore, it has also been shown that whilst polar molecules tend to form a complex hydrogen bonding network with the hydroxyl surface, the polar functional group does not affect the interaction between the organic and the siloxane surface, thus the polar molecules interact similarly with the siloxane surface as that of their non-polar counterpart.[19]

In contrast to quantum mechanical methods, classical molecular dynamic and Monte Carlo simulations can sample a larger range of phase space, and have been able to model the effects of a multitude of organics on solvated kaolinite surfaces. Recent results have concluded that, for example, certain organic molecules (cationic dyes) have a preference to adsorb to the siloxane, rather than the hydroxyl surface,[20] in disagreement with most DFT studies based on energy analyses.[18,19] The study noticed the formation of organic aggregates on the siloxane surface after 10 ns, a timescale untenable to *ab-initio* calculations at this point in time.

In the previous work by the current authors, the interactions of organic matter with smectite clay surfaces at various salinities had been investigated.[21] The work presented that

it was the ionic composition of the brine, rather than the salinity itself, that played an important role upon the adsorption of organic matter to mineral surfaces.

The aim of the present study is to model the interactions of small organic molecules with hydrated kaolinite basal surfaces, to ascertain under what conditions small organic materials adsorb to the siloxane and hydroxyl surface. Organic molecules possessing a shared 10 carbon alkyl backbone, but with varying functional groups, have been simulated on kaolinite clay basal surfaces using classical molecular dynamics. The results are pertinent to a range of phenomena dominated by clay-organic interactions. The aim is to gain a fundamental understanding of the effect of the functional group and charge upon the adsorption of the organic molecules to both the siloxane and hydroxyl basal surfaces of kaolinite. In Section 2 the computational model and input parameters are described. The results for decane interacting with the basal surfaces of kaolinite are presented in Section 3.1. The results for decanoic acid and decanoate anions are presented in Sections 3.2 and 3.3 respectively, whilst the results for decanamine and protonated decanamine are presented in 3.4 and 3.5.

2 Computational Details

2.1 Model Setup

The kaolinite unit cell used in this study had the stoichiometry $Al_2Si_2O_5(OH)_4$ (see Figure 3), with initial atomic positions taken from the American Mineralogist Crystal Structure Database,[22,23] and whilst the unit cell possessed zero net charge, the siloxane and hydroxyl surfaces possess a slight net negative and positive surface charge respectively due to electron polarization (whereby this polarization is implicitly captured by the partial charges on each atom as defined by the utilised force field).

Periodically replicated supercells contained two adjacent sheets of kaolinite composed of 168 unit cells (12 × 7 × 2), with dimensions of approximately 6 × 6 × 10 nm, with each pair of layers separated by a nanopore spacing of approximately 9 nm. The kaolinite
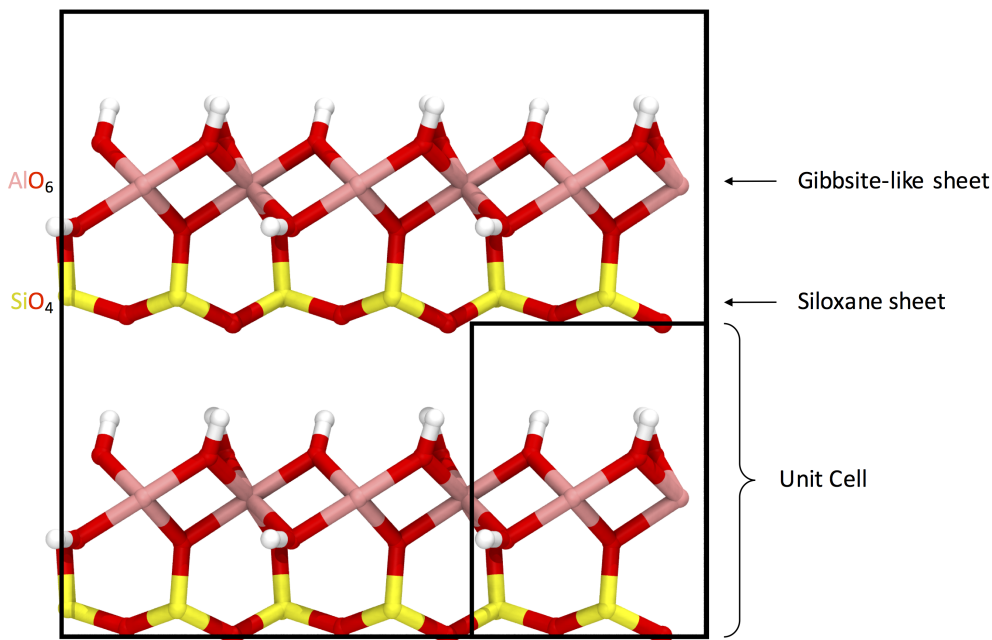
Figure 3: The unit cell of Kaolinite used in this study. The clay structure contains silicon (yellow), oxygen (red), aluminum (pink), and hydrogen (white) atoms.

structures initially occupied the region $0 < z < 1.2$ nm in all models, and the clay position varied little over all timescales modelled. Two hundred organic molecules were subsequently positioned near the hydroxyl and siloxane surfaces, one hundred within 1 nm of the hydroxyl surface, and the other hundred within 1 nm of the siloxane surface, as to increase clay-organic interactions and reduce phase-space sampling time.[21] This was achieved using the program PackMol,[24] resulting in a system similar to that presented in Figure 4. The system was subsequently solvated with (approximately 9000) water molecules to recreate hydrous conditions. It has previously been shown that the organic molecules considered in this study adsorb to the mineral surface when simulated in vacuum.[21]

The organic molecules considered in this study were neutral non-polar decane ($C_{10}H_{22}$), polar decanoic acid ($CH_3(CH_2)_8COOH$) and decanamine ($CH_3(CH_2)_8NH_2$). Additionally, pH effects were considered by altering the protonation state of the decanoic acid and decanamine. Decanoic acid has a pK_a of approximately 4.9,[25] and is likely to be found in both neutral and anionic forms in the majority of natural settings. In contrast, the pK_a

Figure 4: A snapshot showing the initial model of decane interacting with kaolinite before water is added. The PackMol software package[24] has been used to create the densely packed organic phase adjacent to the siloxane and hydroxyl surfaces. All simulations start with similar configurations. The clay structure contains the same color scheme as in Figure 3, whilst the oil molecules contain carbon (blue) and hydrogen (white).

of decanamine is approximately 10.6,[26] meaning that the decanamine will most likely be found in its protonated cationic form in the majority of natural environments, with the notable exception for cementitious materials or drilling fluids where alkaline conditions exist. The following simulations where all decanamine molecules are neutral are unlikely to be encountered in most environmental conditions but a portion of the population of decanamine molecules will be neutral and thus the simulations provide a useful proxy for comparison. Both decanoate $CH_3(CH_2)_8COO^-$ and protonated decanamine $(CH_3(CH_2)_8NH_3^+)$ have been simulated, whereby the charge of the system has been subsequently charge-balanced by the addition of sodium and chloride ions respectively. All organic molecules used in this study were created using the Avogadro molecular editing suite.[27]

In this study it has been assumed that the charge of the clay basal surface remains pH independent. Whilst it has recently been shown that the surface charge of kaolinite is pH

dependent, it can be difficult to decouple how much of this effect is due to basal surfaces or clay edge sites.[28] It has also been shown that between pH values of approximately 6 and 10 the hydroxyl surface remains net neutral.[28,29] The force fields utilised in this study have not been parameterized to model pH imbalances on mineral surfaces, however this topic is currently being considered and is subject to future work.

The ClayFF force field[30] has been used to model the kaolinite clay mineral within the simulations. The force field has been specifically parameterized to model clay-like minerals, and is described wholly through non-bonded Lennard-Jones and Coulomb potentials (with the exception of bonded hydroxyl groups within the clay structure). The CHARMM36 force field[31,32] was utilized to model the organic oil molecules within the clay nanopore. The force field was designed to describe organic systems, and has been proven to reproduce physically accurate representations of hydrocarbons, lipids and similar organics.[33] The CHARMM36 TIP3P water model was used to simulate the water molecules between clay mineral layers. Although ClayFF has been parameterized consistently with the SPC water model, it has since been shown that the force field equally produces qualitatively accurate results when used in conjunction with the CHARMM36 TIP3P water model.[34] Both ClayFF and CHARMM36 force fields have recently been tested in conjunction, and have been shown to accurately reproduce the equilibrium properties of organic molecules interacting with hydrated mineral surfaces.[34] Previous simulations have been able to show that the adsorption of, for example, acetate and ammonium molecules parameterized with CHARMM, to quartz surfaces parameterized with ClayFF, are not only consistent with *ab-initio* molecular dynamics, but also with experimental X-ray reflectivity (XRF) data.[35] Both the quantity and length of hydrogen bonds between the organic molecules and mineral surface agreed within error to both DFT and XRF data. Lorentz-Berthelot mixing rules for van der Waals interactions are utilised in both CHARMM36 and ClayFF force fields, and have been used here to model the intermolecular organic-clay interactions.

2.2   Simulation Details

All simulations were performed using the molecular dynamics suite, GROMACS 4.6.7.[36,37] All simulations were run using real-space particle-mesh-Ewald (PME) electrostatics and a van der Waals cutoff of 1.2 nm. Each simulation was initialized with an energy minimization using a steepest descents algorithm, with convergence achieved once the maximum force on any one atom was less than 100 kJ mol^{-1} nm^{-1}. Subsequently, simulations were run for a 50 ps equilibration period in the constant number of particles, pressure and temperature (NPT) ensemble with a velocity-rescale Berendsen thermostat, temperature coupling constant set to 0.1 ps, and a semi-isotropic Berendsen barostat, with pressure-coupling constant 1 ps. The Berensden thermostat and barostat offered swift equilibration of the system, and convergence was validated as the d-spacing and potential energy converged. The use of a semi-isotropic barostat allowed computationally efficient decoupling of volume fluctuations in the z direction and xy plane. This equilibration simulation was followed by a 50 ns production run in the NPT ensemble using a velocity-rescale thermostat, with a temperature coupling constant of 1 ps, and a semi-isotropic Parrinello-Rahman barostat, with a pressure coupling constant of 1 ps. All simulations were run at approximately ambient conditions, a pressure of 1 bar and a temperature of 300 K. It was necessary to run simulations at ambient, as the ClayFF force field has been parameterized to model systems at room temperature, and considerable validation would be needed to ensure it accurately reproduces structures and properties at various other temperatures and pressures.

2.3   Analysis Techniques and Visualization

All subsequent snapshots of simulation trajectories have been produced using VMD 1.9.2.[38] All simulations contain two adjacent kaolinite layers, which have been reproduced twice in all snapshots at the left and right of the figures. The clay layers are identical and are periodic images of one another. The color scheme of all snapshots are defined as follows. The clay structure contains silicon (yellow), oxygen (red), aluminum (pink), and hydrogen

13

(white) atoms. Organic molecules contain carbon (light blue), hydrogen (white), oxygen (red) and nitrogen (dark blue). Ions are represented as van der Waals spheres and consist of sodium (blue) and chloride (red) ions. Unless otherwise specified this color scheme is kept consistent. Water molecules are present in all simulations, but are not rendered in the snapshots for clarity.

Atomic partial densities across the nanopore were calculated using the built-in analysis tools within GROMACS 4.6.7, and subsequently plotted using Python and MatPlotLib. All density profiles have been averaged over the final 5 ns of the 50 ns production run, and have been subsequently integrated and re-scaled such that the maximum peak in partial density is set to one, in an attempt to increase clarity. The zero in the z-distance of the density plots correspond to the siloxane surface of the kaolinite clay mineral.

The average end-to-end molecular angle has been calculated using the MDAnalysis[39] Python library. The angle of an organic molecule is defined *via* the vector generated between CH_3 carbon and the final carbon (or nitrogen for decanamine) on the opposing molecular functional group. For decane, the choice between head and tail end of the vector is arbitrary. Each organic molecule generates one vector, and the orientation of this organic is measured in spherical coordinates over the final 5 ns of the 50 ns production simulation. The convention used in the present work is such that the clay mineral sheet lies upon the xy plane, and the azimuthal angle is defined as the angle around the z axis upon the clay plane, originating from the x axis, see Figure 5 (left) for a schematic. The elevation angle is thus defined as the orientation above or below the xy plane and therefore above or below the clay mineral. A positive elevation angle means that the functional group of an organic points away from the hydroxyl surface and toward the siloxane surface, whilst a negative elevation angle represents the opposite molecular orientation. See Figure 5 (center) and Figure 5 (right) for a schematic representation of a vector with positive and negative elevation angles respectively.
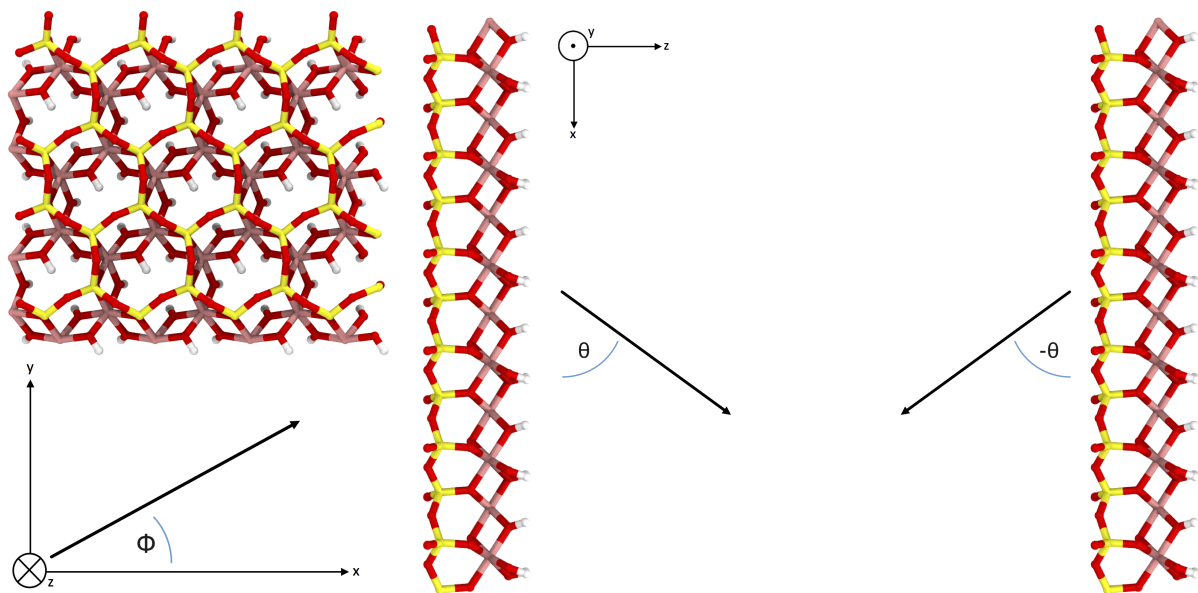
Figure 5: A schematic of angles definitions. The azimuthal angle (left) is defined as the angle on the xy plane, about the z axis. The elevation angle (right) is defined as the angle above or below the xy plane, and thus above or below the basal surface of the clay.

3 Results & Discussion

3.1 Interactions of Decane with Kaolinite

Decane forms the backbone of all the subsequent organic molecules tested, and the behaviour observed for decane is expected to play a role in the mechanics of the other simulations. The simulation results show complete organic molecule withdrawal from the hydrophilic hydroxyl surface, with organic adsorption to the hydrophobic siloxane surface, as is clear from the final snapshot of the simulation in Figure 6. This process occurs very rapidly. After a 50 ps equilibration period both oil aggregates have formed clear droplet structures, with the hydroxyl droplet already withdrawn from the surface, see Figure 7 (top). After a few nanoseconds, the two oil droplets coalesce and form the single droplet observed in the post-production snapshot, Figure 7 (bottom).
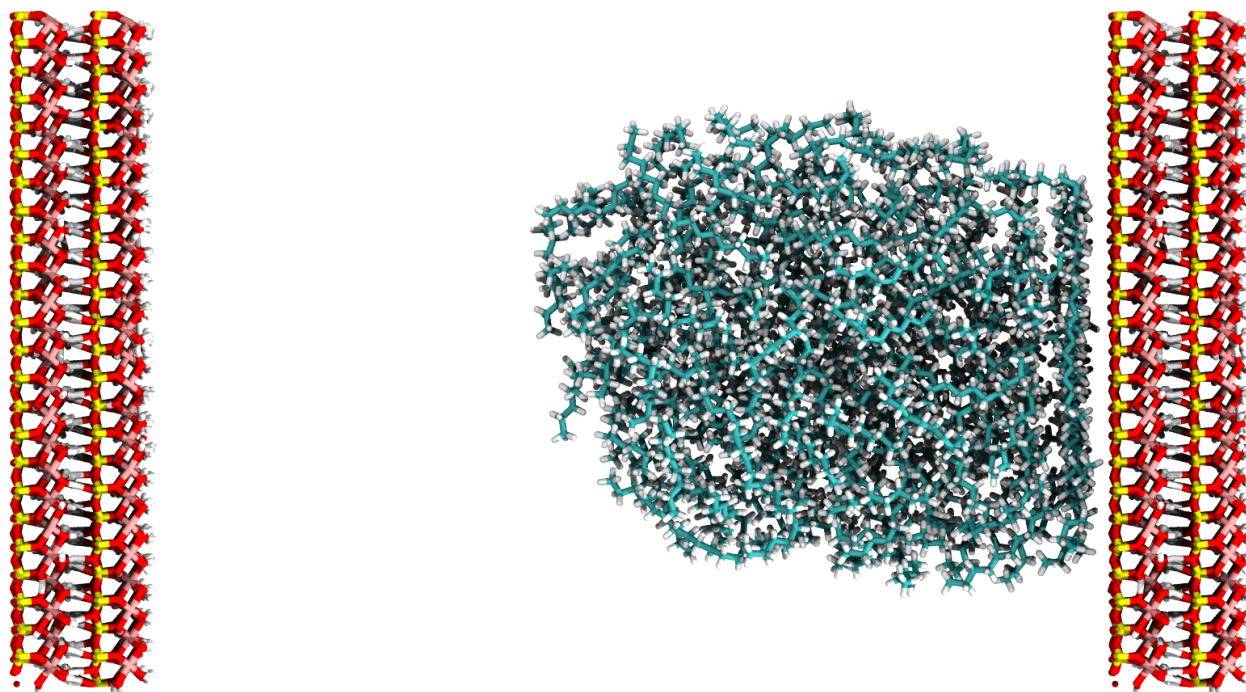

Figure 6: The post-production snapshot of decane interacting with kaolinite. Note the complete withdrawal of decane from hydroxyl surface and adsorption to siloxane surface.

Figure 8 (top) presents the partial density profile of decane molecules across the pore spacing. It can be seen that the organics nearest the siloxane surface of the kaolinite form
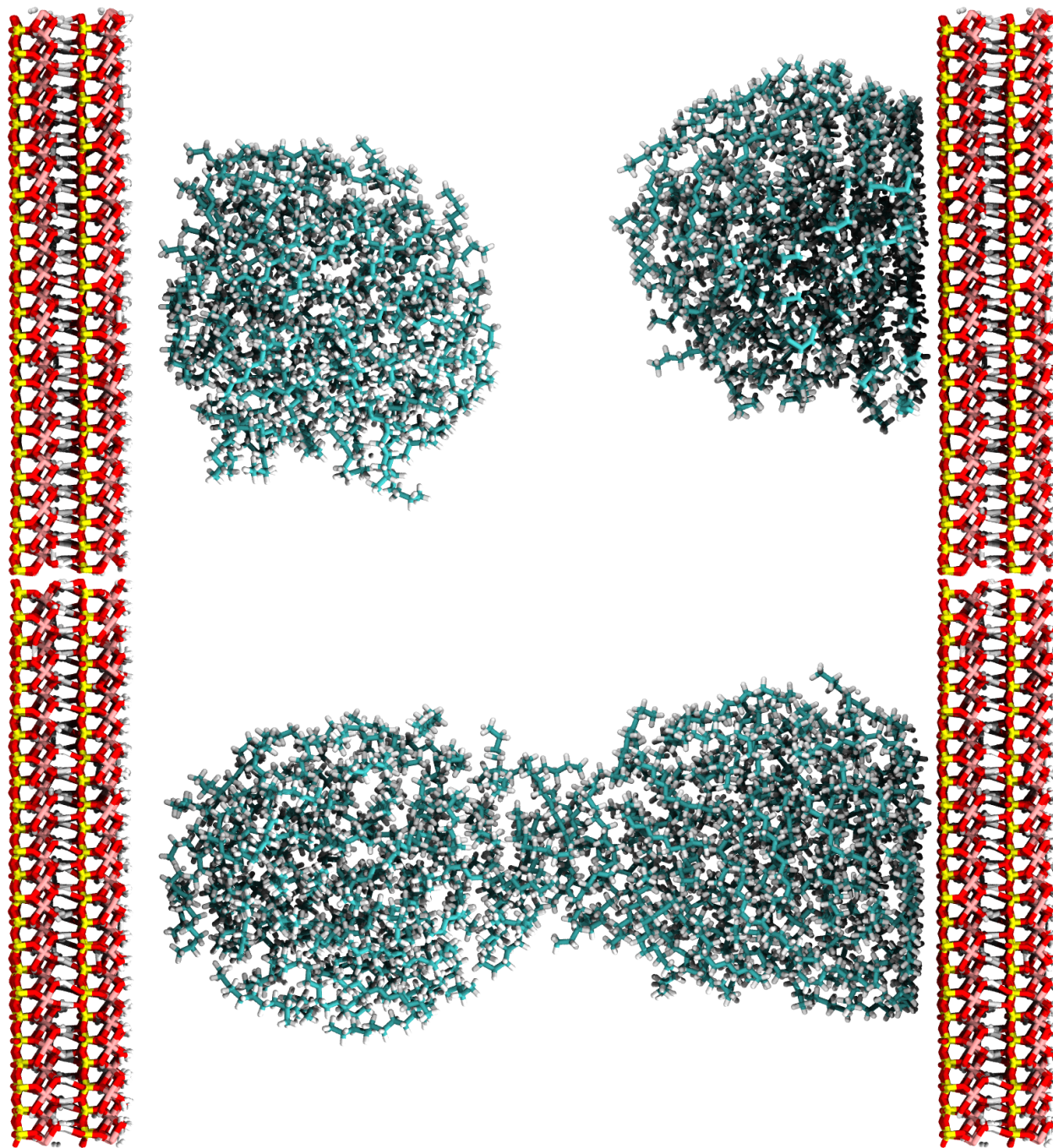
Figure 7: Simulation snapshots of decane interacting with kaolinite at various times throughout the simulation. The upper snapshot presents the rapid formation of two separate oil droplets after the 50 ps equilibration period, whilst the lower snapshot presents the two oil droplets coalescing after 2 ns. Following this process, the oil droplet remains adsorbed to the siloxane surface.

discrete layers parallel to the plane of the surface. The results suggest that the organics near the surface lie horizontally and stack upon one other, this effect can also be observed slightly in Figure 6. Further work shall examine how the phenomena originates, comparing the average oxygen-oxygen distance of the siloxane surface and determining whether this correlates to the carbon-carbon or hydrogen-hydrogen separation of the oil. In previous work, Swadling *et al.*[40,41] and Thyveetil *et al.*[42,43] have observed coupling between molecular alignment and the thermal undulations within layered minerals, though these are less likely in kaolinite owing to the thickness of the double repeat used in these simulations.
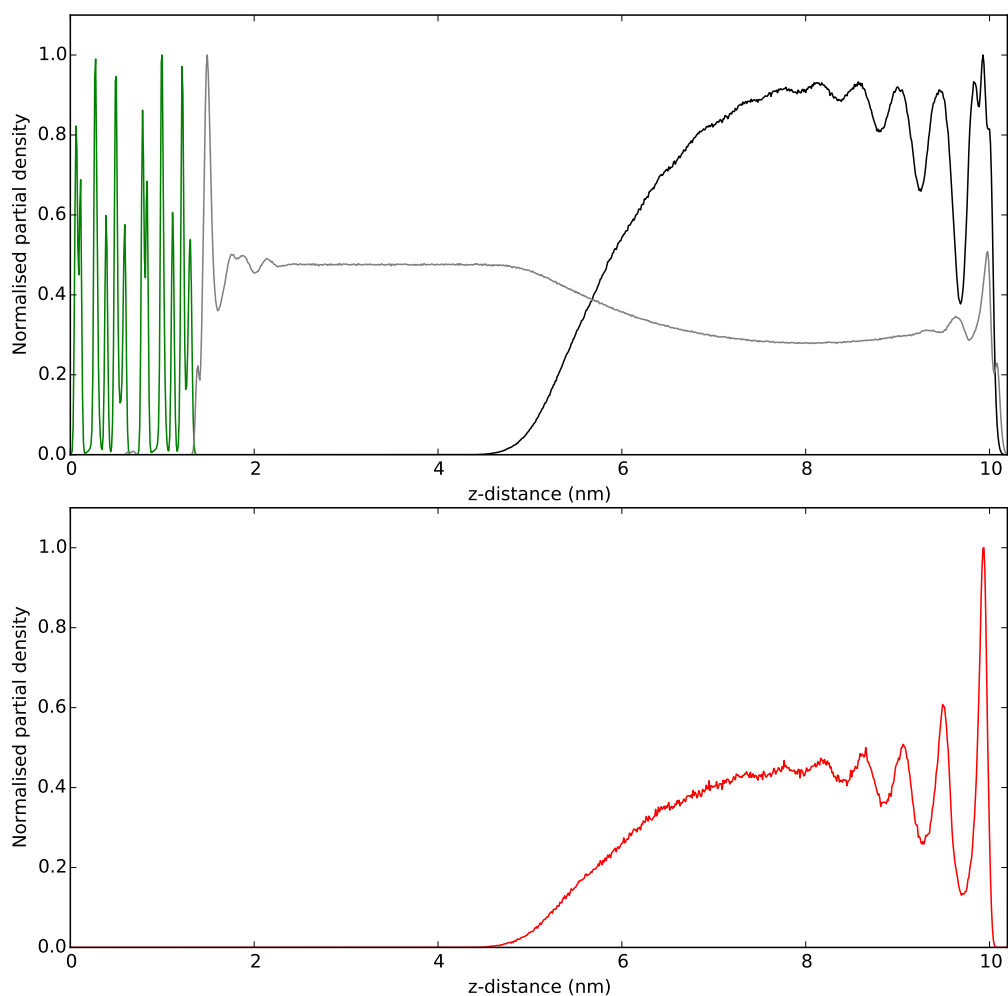

Figure 8: The re-scaled density profiles of decane across the pore spacing. The top subfigure presents all components in the system, kaolinite (green), water (grey) and decane (black). The lower subfigure presents the density profile of CH_3 carbon's within the functional groups of decane.

18

Figure 8 (bottom) presents the partial density of CH_3 carbons within the pore spacing. Again it is clear that the CH_3 groups form well ordered layers adjacent to the clay. Due to the symmetry of decane, neither end of the molecule has a larger binding affinity to the clay surface, nor possess differing hydration enthalpies, and it is not surprising that the saturated alkanes lie parallel to the plane in this instance.

The first peak in the decane partial density profile is approximately 3.1 Å from the siloxane surface, with subsequent peaks approximately 4.4 Å apart from each other. The simulations present that van der Waals interactions are the primary adsorption mechanism for decane on the siloxane surface, as the electrostatic partial charges of decane are minimal. It is favourable for water, rather than decane, to hydrate the surface of the clay mineral, establishing extensive hydrogen bonding with the hydroxylated surface. Overall, van der Waals interactions between decane and the clay surface are responsible for organic adsorption to the siloxane surface, whilst the preferential hydrogen bonding between water and the clay surface is responsible for the withdrawal of decane from the hydroxyl surface.

Figure 9 (left) presents the angle distribution for decane molecules within the kaolinite nanopore. Note the fairly large spread of organic molecule orientation, however, also note that some organic molecules possess a favourable orientation at an elevation angle of 0 rad, i.e. parallel to the kaolinite surface, and an azimuthal angle of $+\pi/3$ rad and $-2\pi/3$ rad.
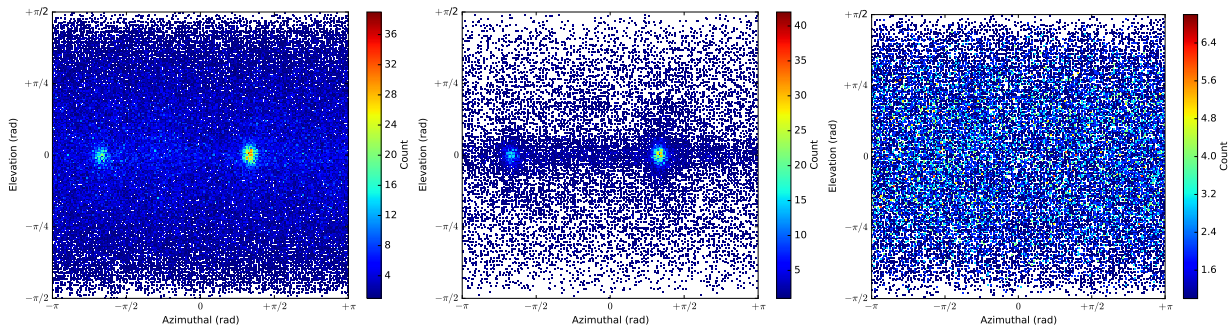

Figure 9: The angle distribution of all decane molecules in the pore spacing (left), decane molecules within 0.5 nm of the siloxane surface (center) and decane furthest from the clay surface, at least 3 nm from surface (right).

Figure 9 (center) presents the orientation of the organic subset closest to the siloxane

surface, i.e. all organics within the first density peak in the density profile of Figure 8 (z >
9.5 nm). There is a strong relationship between the elevation angle of an organic and its
proximity to the basal surface. The azimuthal angle is heavily biased toward $+\pi/3$ rad and
$-2\pi/3$ rad. These angles correspond to opposing directions, hence the organics lie along
the same axis of symmetry. This axis of symmetry happens to be one of the hexagonal
axes of symmetry of the siloxane surface, and to be specific, it pertains to one of the axes
of symmetry of basal oxygens. The results present that the organics closest to the surface
not only lie horizontally, but also tend to lie along one of the siloxane axes of hexagonal
symmetry. Further work shall examine the origin of this ordering phenomenon, comparing
the average oxygen-oxygen distance of the siloxane surface and determining whether this
correlates to the carbon-carbon or hydrogen-hydrogen separation of the oil.

Figure 9 (right) presents the angle profile of decane molecules furthest from the siloxane
surface (z < 7 nm in Figure 8). This subset of adsorbed organics possesses no prejudice
to azimuthal angle. The orientation of organics is distributed evenly, and the organics are
oriented as though the clay minerals were not present.

3.2   Interactions of Decanoic Acid with Kaolinite

Decanoic acid is still dominated by the alkane chain and thus might be expected to behave
similarly to decane, however, the role of the hydrophilic COOH group is considered to alter
the behaviour of organic-clay and organic-water interactions. Figure 10 (top) presents a post-
production snapshot of decanoic acid interacting with kaolinite. Again, when compared to
the starting configuration in Figure 4, it is clear that organics readily withdraw from the
hydroxyl surface and adsorb on the siloxane surface. Note that the decanoic acid forms a
less broad droplet compared to decane, indicating that the polar functional groups act as to
increase the contact angle, and thus interfacial tension, of the oil phase. Upon rotating the
system, the simulations present that the droplet additionally acts as a film across the clay
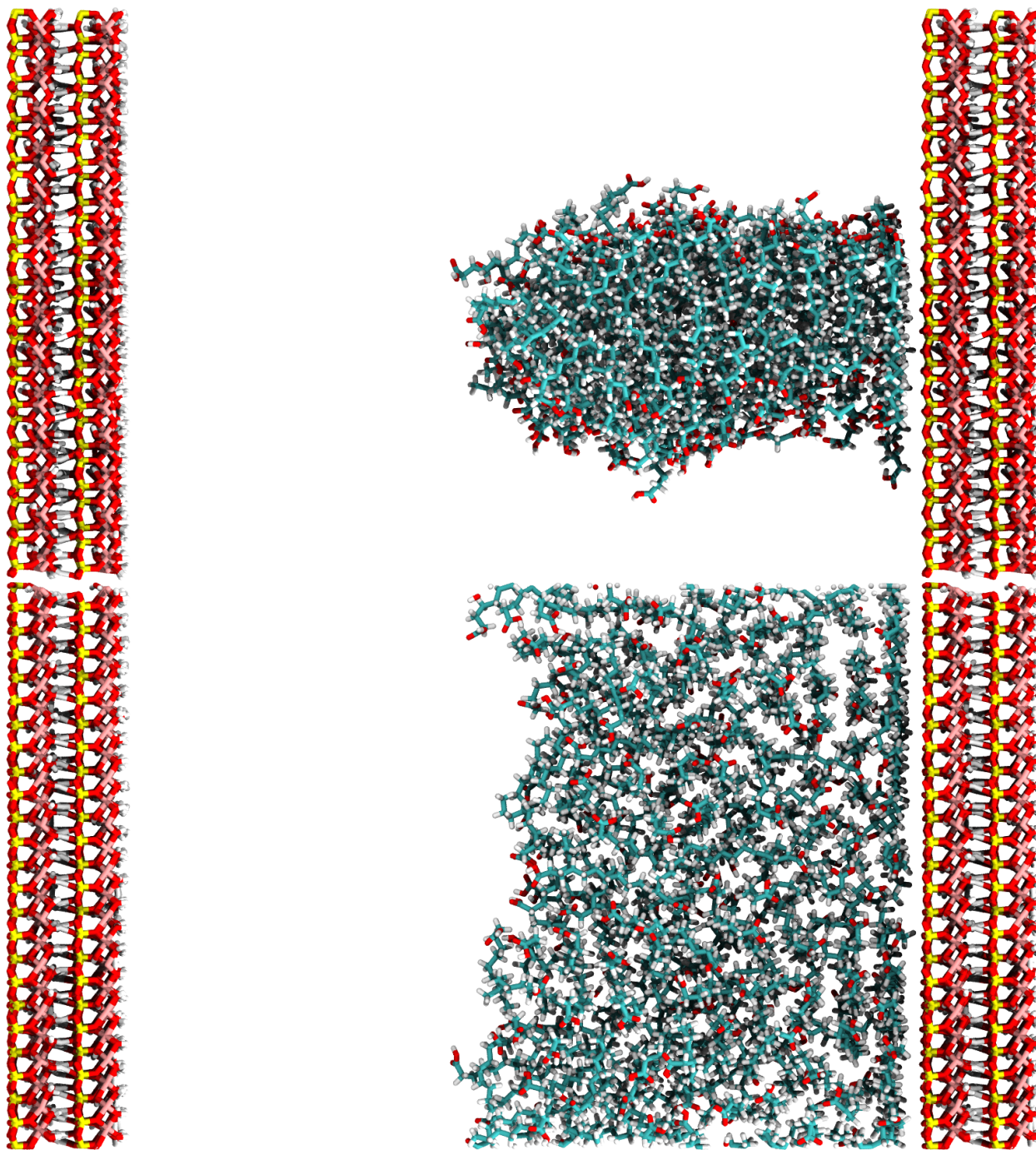surface, see Figure 10 (bottom).

Figure 10: Post-production snapshots of decanoic acid interacting with kaolinite (top and bottom rotated through 90°). Note the complete withdrawal of the organic from hydroxyl surface, with adsorption to siloxane surface, much like decane, Figure 6.

Figure 11 (top) presents the density profiles of the clay, organic molecules and water across the pore space. As with decane, the decanoic acid molecules form horizontal layers close the siloxane surface, and the effect of the COOH functional group appears to be minimal to the overall adsorption behaviour of decanoic acid. Figure 11 (bottom) shows the partial
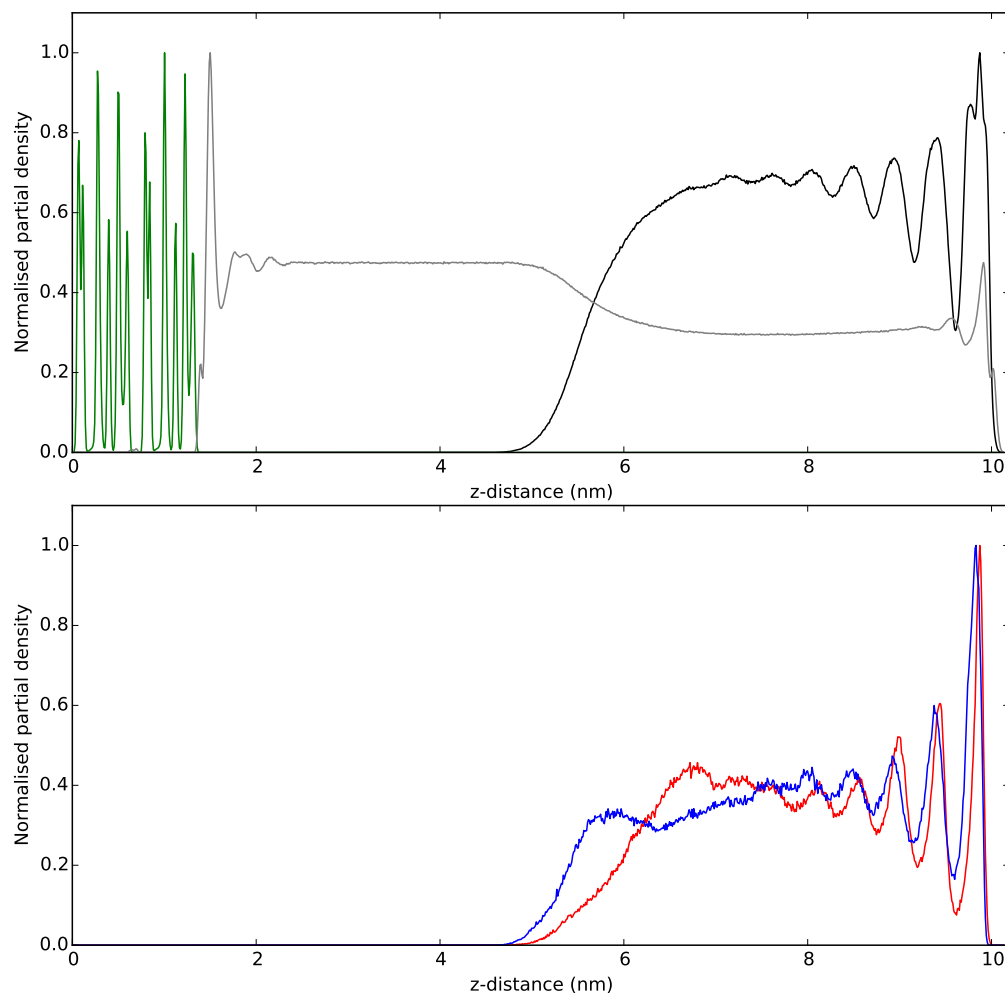

Figure 11: The re-scaled density profiles of decanoic acid across the pore spacing. The top subfigure presents all components in the system, kaolinite (green), water (grey) and decanoic acid (black). The lower subfigure presents the density profile of CH_3 carbons (red) and COOH carbons (blue) of the decanoic acid molecules within the nanopore.

densities of CH_3 and COOH functional groups across the pore space. It can be seen that in close proximity to the clay surface, the behaviour of CH_3 and COOH is very similar. The density of COOH appears to reach further into the pore spacing compared to CH_3 however. This is due to the hydrophilic nature of the COOH functional groups; it is favourable for the

organic cluster to create a micelle-like structure on the clay surface, minimising hydrophilic-hydrophobic interactions between CH_3/CH_2 groups in the decanoic acid with water.

The first peak distance between the clay surface and the CH_3 functional group is again 3.1 Å, whilst the distance between surface and the COOH functional group is 3.4 Å. Further peaks are separated by approximately 4.4 Å for both CH_3 and COOH. Again, the primary adsorption mechanism seen here is van der Waals interactions between organic and siloxane surface.

As with the decane simulations, no interactions between hydroxyl surface and organic molecules are observed. The results confirm that the binding affinity of the water phase is greater than that of the polar COOH group, and that the hydroxyl surface is readily hydrated by water in preference to decanoic acid. In contrast, the binding affinity of the hydrocarbons on the siloxane surface is greater than the hydration energy of water on the same siloxane surface.

Figure 12 (left) presents the angle analysis for all decanoic acid molecules within the kaolinite pore. The organic molecules generate a very distinctive concentric elliptical distribution of angles, very dissimilar to that observed for decane, Figure 9. Figure 12 (center) again presents the orientation of the organics closest to the clay, i.e. all organics within the first peak in the density profile of Figure 11 (z > 9.5 nm). Note that the organics lie azimuthally along one of the hexagonal axis of symmetry of the siloxane surface (once again, in line with basal oxygen atoms), at an angle of $+\pi/3$ rad and $-2\pi/3$ rad. The two primary nodes (the areas of highest angle concentration) are centred upon the xy plane, i.e. where the elevation angle is zero, and thus the majority of the organics lie horizontal to the siloxane surface. Figure 12 (right) presents the angle profile of decanoic acid molecules furthest from the siloxane surface (z < 7 nm in Figure 10). It can be seen that the organics maintain a preferential orientation, with the carboxylic acid heads pointing into the pore spacing (negative elevation), thus increasing polar-polar interactions between organic and solvent. The preference in azimuthal angles is due to the cylindrical droplet formation of the

organics at the surface. The polar functional groups have a marked effect on the orientation of the organics far into the pore spacing, a phenomenon that is not observed in the decane simulations.
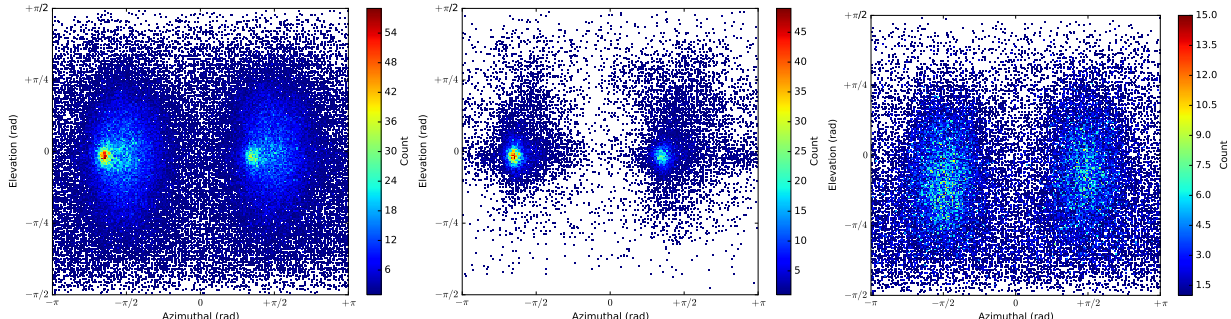

Figure 12: The angle distribution of all decanoic acid molecules in the pore spacing (left), organic molecules within 0.5 nm of the siloxane surface (center) and decanoic acid molecules furthest from the clay surface, at least 3 nm from surface (right).

3.3   Interactions of Decanoate Anions with Kaolinite

The deprotonation of decanoic acid is expected to dramatically alter organic-clay behaviour as ionic interactions are far stronger than the hydrogen bonds observed for decane and protonated decanoic acid.[17] Figure 13 presents the final snapshot of the production run of Na-decanoate interacting with kaolinite. The behaviour is comprehensively different to that of decane and decanoic acid. The results show complete organic withdrawal from the siloxane surface, and adsorption to the hydroxyl surface.

It is also worth highlighting, in particular, the distribution and behaviour of the charge-balancing sodium cations. Figure 14 (top) clearly presents the affinity of sodium to adsorb to both the electronegative siloxane and electropositive hydroxyl surfaces of kaolinite. The simulations show that the sodium cations form inner-sphere surface complexes (ISSCs) on the hydroxyl surface and outer-sphere surface complexes (OSSCs) on the siloxane surface. ISSCs are defined as ions directly adsorbed to the surface of a mineral, whilst OSSCs are hydrated ions indirectly adsorbed to the surface *via* a mediating water molecule. One may think that ISSCs are inherently more strongly bound to a clay surface, whilst OSSCs in
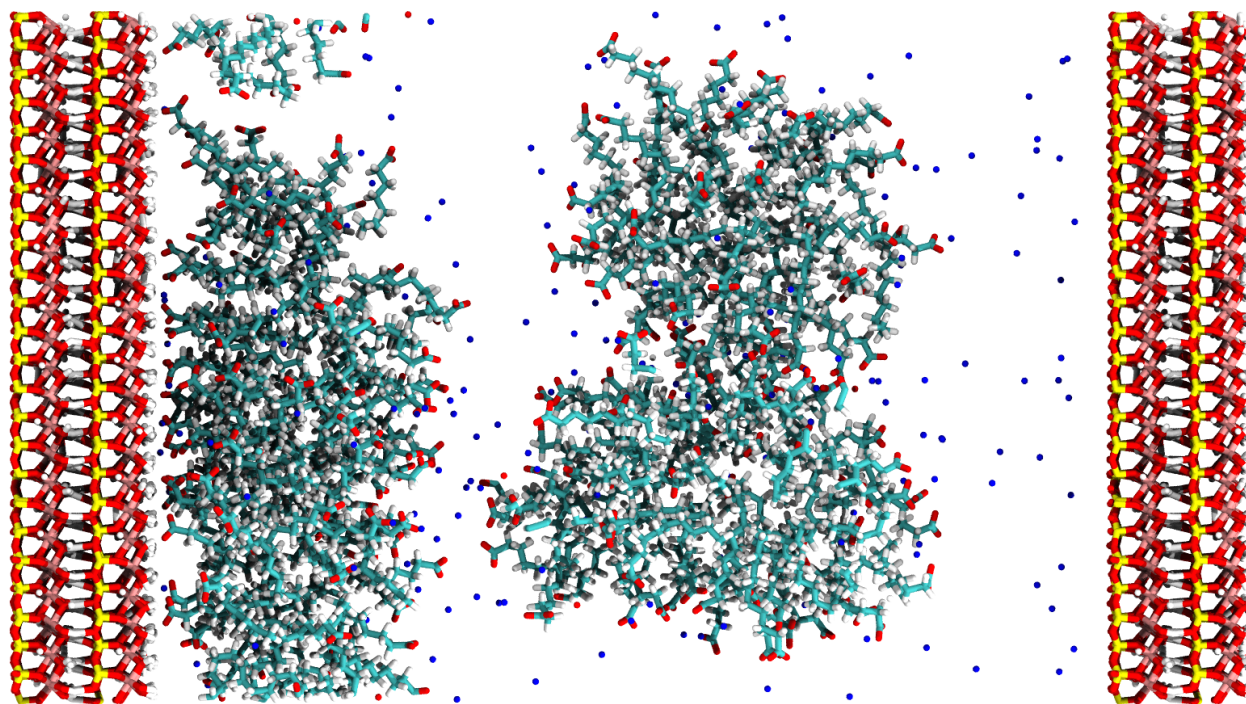
24

Figure 13: The post-production snapshot of Na-decanoate interacting with kaolinite. Note the stark difference in behaviour compared to protonated decanoic acid (Figure 10), *viz* complete withdrawal from the siloxane surface yet adsorption to hydroxyl surface.

comparison are less strongly bound to a mineral surface, however this has recently been shown to not necessarily be true, and any conclusions drawn from the behaviour ISSC versus OSSC must be considered on a case-by-case basis.[44] The result is surprising however, not only are sodium ions able to adsorb to the electronegative siloxane surface, but also the electropositive hydroxyl surface. The sodium adsorption to the hydroxyl surface may be ascribed to ionic interactions between cations and atoms further within the clay mineral, for example the gibbsite oxygens or aluminums, whilst the phenomenon may also be described by the presence of the negatively charged organic matter.

Figure 14 (top) also presents the density profile of the decanoate molecules in the pore spacing. The profile shows two distinct regions of organic aggregation, one set of organics adsorbed to the hydroxyl surface of the clay and a separate cluster *floating* within the pore spacing. The partial densities show that the charged organics withdraw readily from the siloxane surface, and do not interact with the clay surface thereafter. No occurrence of
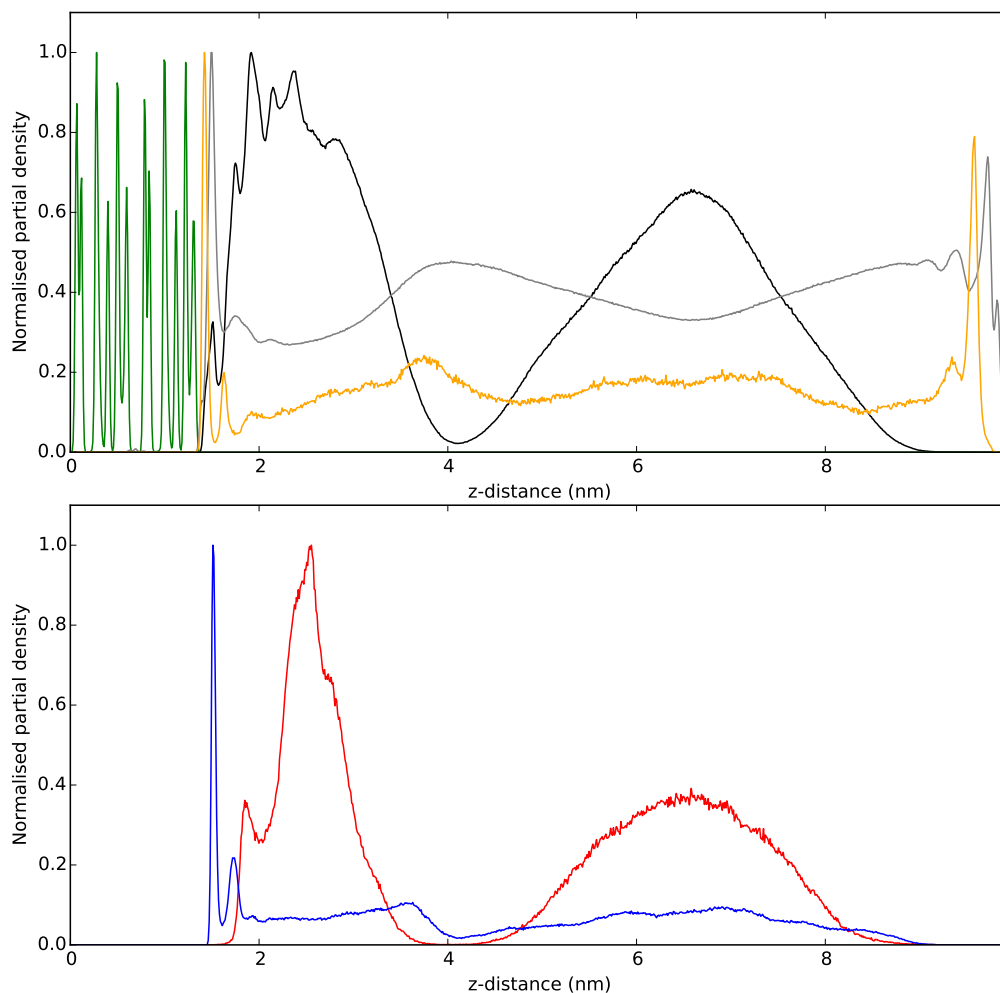
Figure 14: The re-scaled density profiles of Na-decanoate across the pore spacing. The top subfigure presents all components in the system, kaolinite (green), water (grey), decanoic acid (black) and charge balancing sodium ions (orange). The lower subfigure presents the density profile of CH_3 carbons (red) and COO^- carbons (blue) of the decanoate anions within the nanopore.

cation bridging between siloxane and decanoate is observed here, a result that is consistent with previous observations of the siloxane surfaces in 2:1 smectite clays.[21] The decanoates initially adjacent to the hydroxyl surface remain adsorbed throughout the 50 ns production run *via* an anion exchange mechanism.

Figure 14 (bottom) presents the distribution of the decanoate CH_3 and COO^- groups within the nanopore spacing. It is clear from the Figure that the COO^- functional groups mediate the organic adsorption to the hydroxyl surface, whilst the CH_3 groups play a minimal

role.

Figure 15 (left) presents the angle profile of decanoate organics adsorbed to the hydroxyl surface ($z < 4$ nm). There appears to be little trend in the angle distribution, which suggests that organics point in all directions. A slight preference for the elevation angle to be aimed toward $-\pi/2$ rad relates to the attraction between charged functional groups and the sodium ions adsorbed to the hydroxyl surface. Figure 15 (right) presents the angle distribution of organic molecules floating within the pore spacing. It can be seen that the organics orientate randomly, as expected of a spherical aggregate.
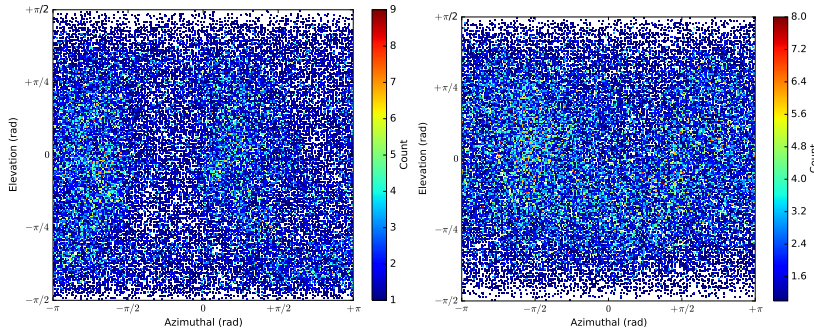

Figure 15: The angle distribution of all Na-decanoate molecules adsorbed to the hydroxyl surface spacing (left), and those floating within the nanopore region (right).

3.4   Interactions of Decanamine with Kaolinite

The effect of introducing NH_2 functional groups can be seen in Figure 16 (top), the post-production snapshot of decanamine on kaolinite. Two separate organic aggregates can be observed in the snapshot, one tightly packed cluster adsorbed to the siloxane surface, and another in close proximity of the hydroxyl surface. Upon rotating the system, Figure 16 (bottom), it can be observed that both aggregates create cylindrical films, one adsorbed directly to the siloxane surface, and one floating above the hydroxyl surface.

The film adsorbed upon the siloxane surface forms clear horizontal layers, similar to the results of uncharged and polar organics previously presented. The film within the pore spacing appears to have withdrawn from the hydroxyl surface, however, the aggregate drifts
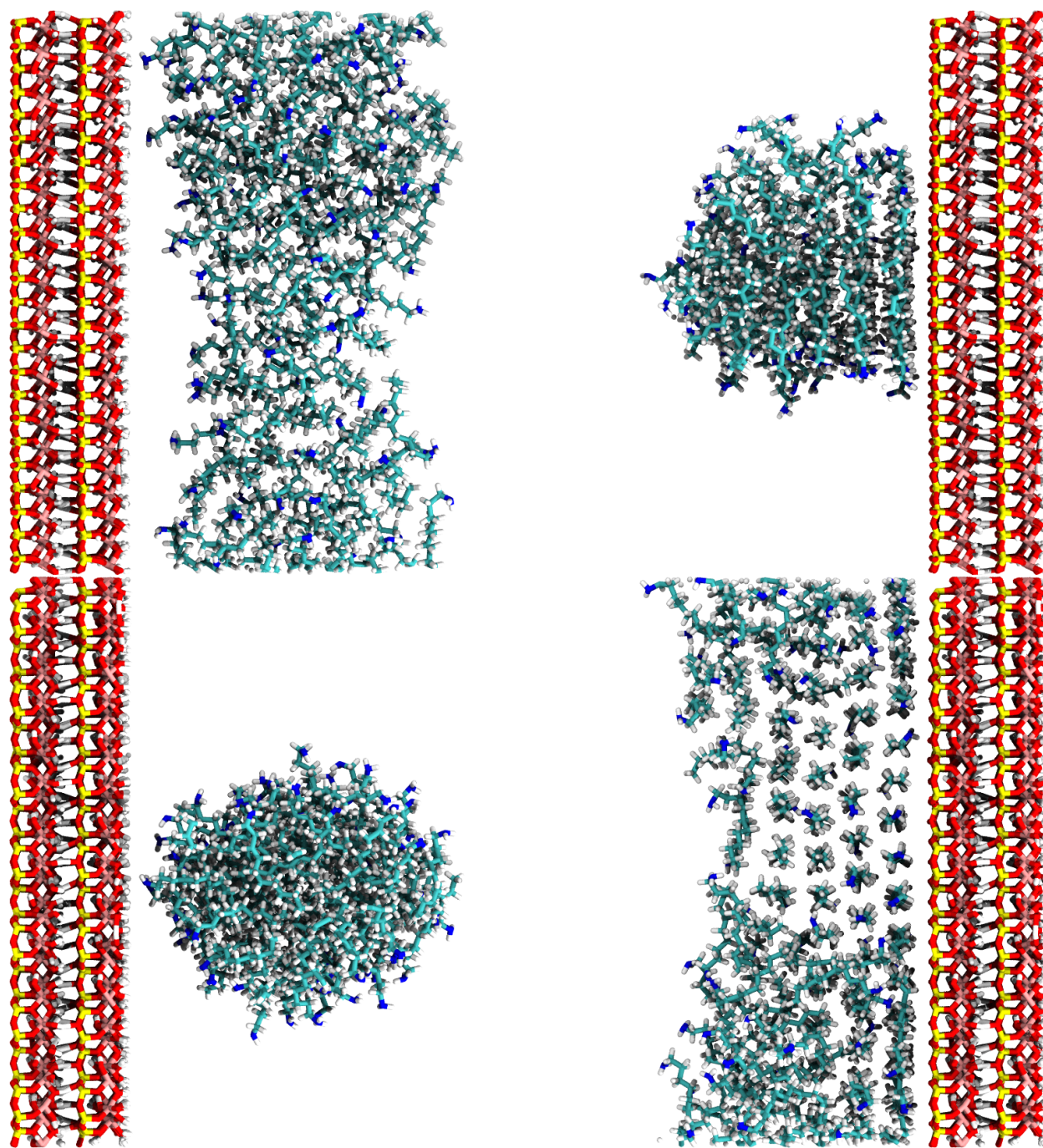
Figure 16: Post-production snapshots of decanamine interacting with kaolinite. Observe the adsorption of organic molecules to both hydroxyl and siloxane surfaces.

very little throughout the simulation, as can be seen from the density profiles, Figure 17 (top). The implication is that the NH_2 functional groups can form strong hydrogen bonds and subsequently form water-bridging networks with the hydroxyl surface.
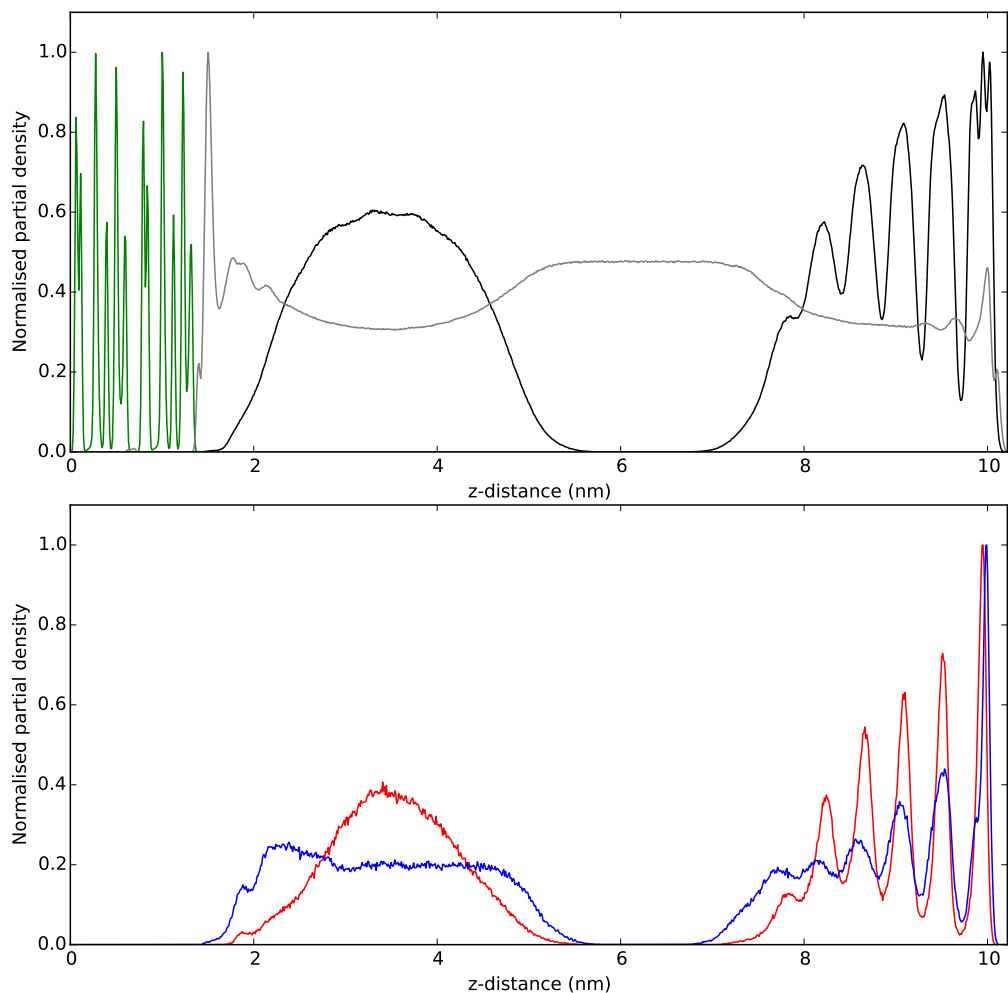

Figure 17: The re-scaled density profiles of decanamine across the pore spacing. The top subfigure presents all components in the system, kaolinite (green), water (grey) and decanamine (black). The lower subfigure presents the density profile of CH_3 carbons (red) and NH_2 nitrogens (blue) of the decanamine molecules within the nanopore.

The partial density profile of CH_3 and NH_2 functional groups are presented in Figure 17 (bottom). The distance between siloxane surface and the first peak of CH_3 and NH_2 is 3.3 Å and 2.8 Å respectively. The increased affinity between surface and NH_2 group is due to the larger degree of polarity in the primary amine compared to CH_3 groups. The large electronegative nitrogen and slightly electropositive hydrogens are thought to create strong

29

N−H $\cdots$ O hydrogen bonds with the surface in comparison to the van der Waals interactions formed by the CH_3 termini. The average distance between density peaks on the siloxane surface is again 4.4 Å, which suggests that the intermolecular interactions between organic molecules is similar for decane, decanoic acids and decanamine. Also note the density profile of NH_2 groups in the cluster near the hydroxyl surface. Here, the NH_2 groups form small density maxima near the hydroxyl surface. In comparison to the water density in Figure 14 (top) it can be seen that the NH_2 maxima lie within the hydration peaks of the clay surface. That is, the NH_2 groups lie between the first and second hydration layer/shell of the hydroxyl surface. The results present the formation of water bridges between clay and organic molecule, however, unlike traditional water-bridging where the interaction is mediated by a strongly solvated ion, here the bridging occurs *sans* salt. The NH_2 functional group is able to form water bridges with the hydroxyl surface through a layer of water molecules. It has previously been observed that the first hydration layer of the hydroxyl surface can be frozen in place,[45,46] and this may explain why such an effect is observed here. The simulations present that NH_2 functional groups can adsorb to both surfaces of the kaolinite clay.

Figure 18 (left) shows the angle distribution amongst the molecules contained within the cluster in close proximity to the hydroxyl surface. The figure presents a slight preference for the polar groups to be pointing toward the hydroxyl surface, inferring that clay-organic interactions exist. There is also a preference for the organics to be orientated at $\pm\pi/2$ rad in the azimuthal plane. This effect is due to the cylindrical structure of the organic droplet in this simulation after 50 ns. Figure 18 (center) presents the angle distribution of decanamine in the organic cluster adsorbed to the siloxane surface. A clear preference for the NH_2 group to point into the pore spacing can be seen. This infers that the NH_2 group is liable to interact with the surrounding solvent, whilst the CH_3 chain ends interact with the hydrophobic siloxane surface. Figure 18 (right) is the angle distribution of organics closest to the siloxane surface, contained within the peak closest to the clay in Figure 17 (z > 9.5

nm). It is clear that the majority of organics lie parallel to the basal surface here, with an elevation angle of 0 rad. The distinct azimuthal pattern observed in Figure 18 (center) can also be seen here, with the majority of organics lying along an azimuthal angle of 0 and $\pm\pi$ rad, and a small portion lying along the azimuthal angle of $-3\pi/2$ rad. All of these axes correspond to one of the hexagonal axis of symmetry of the siloxane surface, as previously discussed.
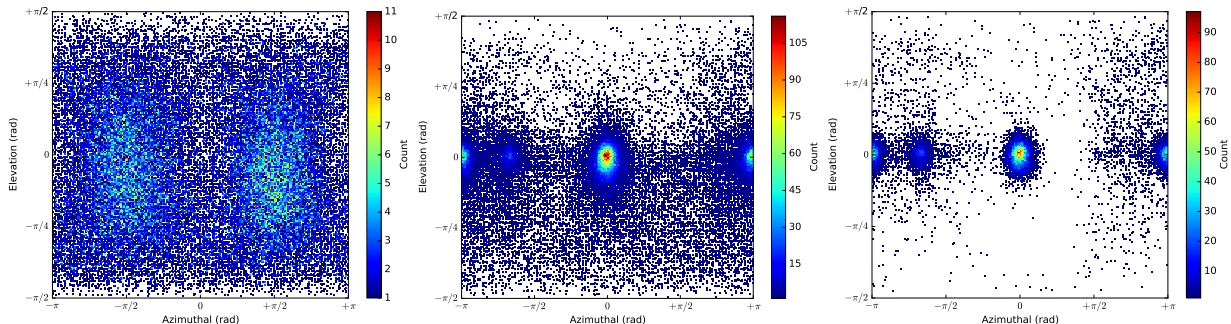

Figure 18: The angle distribution of the decanamine cluster adjacent to the hydroxyl surface (left), decanamine molecules adsorbed to the siloxane surface (center) and decanamine molecules closest to the siloxane surface, at least 0.5 nm from surface (right).

3.5   Interactions of Protonated Decanamine with Kaolinite

Figure 19 is the post-production snapshot of protonated decanamine interacting with kaolinite. Again, two separate organic aggregates can be observed in Figure 19, one adsorbed to the siloxane surface, and another adsorbed to the hydroxyl surface.

Figure 20 (top) is the density profile of protonated decanamine and chloride ions across the pore spacing. Unlike the organic anions in the decanoate simulations, the charge balancing chloride ions only adsorb to the positive hydroxyl layer of the kaolinite surface. The result suggests that the hydroxyl surface will readily adsorb both anions and cations, whilst the siloxane surface will selectively adsorb cations.

The organic molecules adsorbed to the siloxane surface are less ordered compared to the layered structuring observed in the previous simulations. This is due to the ionic repulsion between NH_3^+ functional groups overwhelming the van der Waals and hydrogen bonding
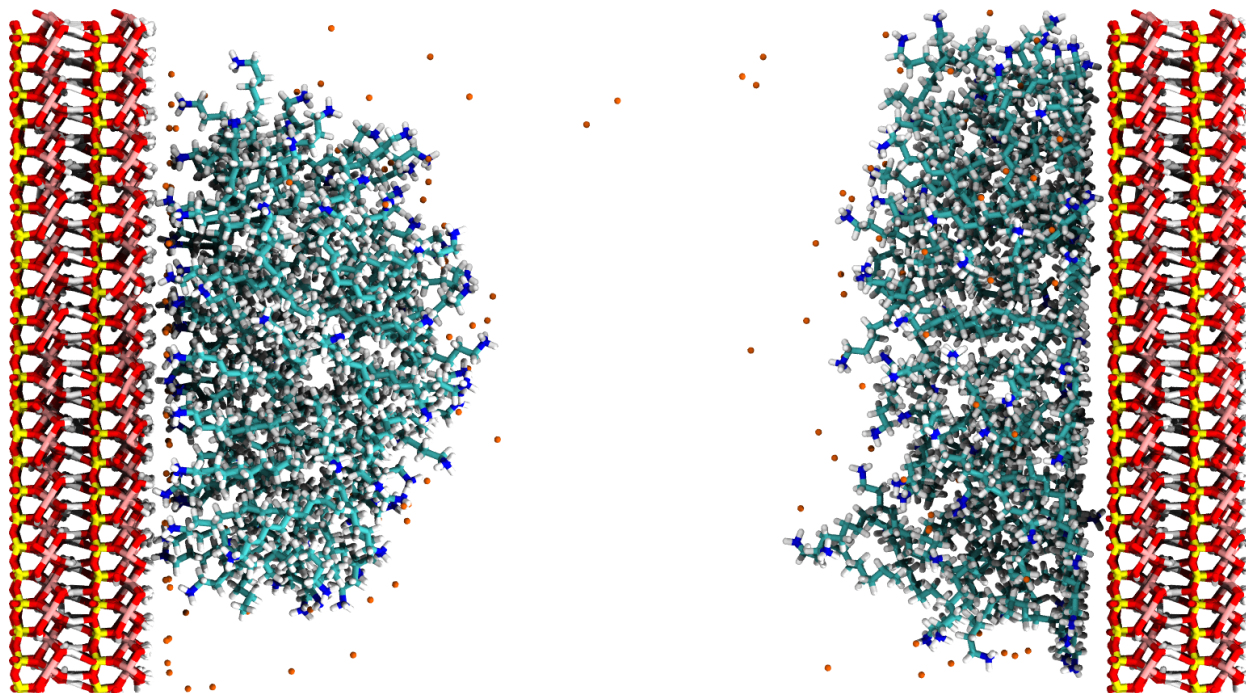
Figure 19: The post-production snapshot of protonated decanamine interacting with kaolinite. Note the difference in behaviour compared to deprotonated decanamine (Figure 16), *viz* adsorption to both siloxane surface and hydroxyl surfaces.

networks previously stacking the organic molecules upon the siloxane layer. Despite this, the layer of organic molecules closest to the clay surface appear to be positioned parallel to the siloxane layer. This orientation then maximises both the ionic interactions between NH_3^+ and the surface as well as the van der Waals interactions between the backbone of the organic and the surface. It can also be seen from the partial density profile of NH_3^+ and CH_3 functional groups, Figure 20 (bottom), that the first layer of organics on the siloxane surface lie parallel to the surface. Beyond this, the organics are less strictly structured, as NH_3^+ functional groups repel one another. The primary adsorption mechanism observed here is cation exchange for NH_3^+ groups, and van der Waals interactions for CH_3/CH_2 backbones.

The adsorption of the organic molecules to the hydroxyl surface is mediated by the small anions within the pore spacing. Note that the chloride ions appear form slight inner-sphere surface complexes, suggesting that the primary adsorption mechanism is anion bridging in this instance. This is a mechanism that is not well described in literature, as it is thought to
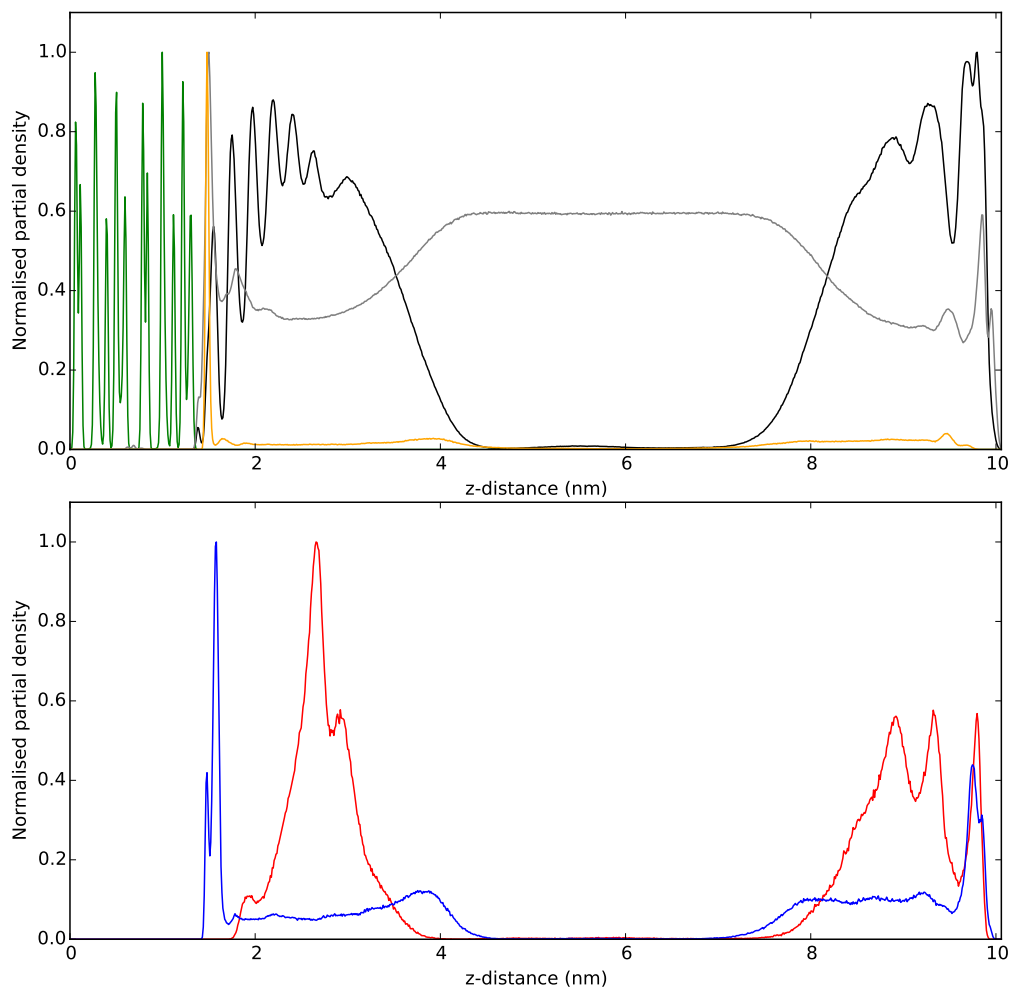
Figure 20: The re-scaled density profiles of protonated decanamine across the pore spacing. The top subfigure presents all components in the system, kaolinite (green), water (grey), decanamine (black) and charge balancing chloride ions (orange). The lower subfigure presents the density profile of CH_3 carbons (red) and NH_3^+ nitrogens (blue) of the protonated decanamine molecules within the nanopore.

be too weak and short lived to play a significant role in the structure of kaolinite surfaces. As previously noted, it is thought that anion bridging occurs primarily on positively charged hydroxide minerals (layered double hydroxides), and is short-lived as the anions are readily replaced by water molecules.[16] The presented results here show that anion bridging is not only possible, but also occurs in 1:1 clays, in addition to layered hydroxide minerals.

Figure 21 (left) presents the angle distribution of organics adsorbed to the hydroxyl surface of the kaolinite clay ($z < 5$ nm). The figure presents no clear preference for azimuthal direction of organics, however a clear trend in elevation can be seen. The organics tend to

face either directly toward or away from the clay surface, at an angle of $-\pi/2$ or $+\pi/2$ respectively. The result suggests that the NH_3^+ functional groups are directly causing the adsorption of decanaminium to the hydroxyl surface. Figure 21 (center) shows the angle distribution for the organics adsorbed to the siloxane surface. It can be seen that there is a preference for the organics to lie horizontal to the basal plane, and a slight preference for the NH_3^+ functional groups to point into the pore spacing. Figure 21 (right) presents the angles of organics nearest the siloxane surface (z > 9.5 nm) and also shows an indistinct azimuthal preference. However, it is clear from the figure that the NH_3^+ groups point directly toward the clay. Figure 21 (right) presents that the protonated decanamine molecules are ionically attracted to the siloxane clay surface, forming cation exchange adsorption sites.
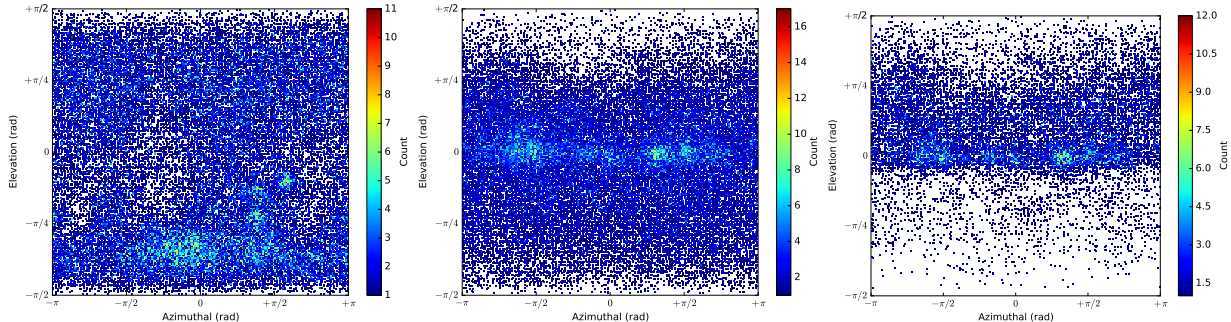

Figure 21: The angle distribution of protonated decanamine molecules adsorbed to the hydroxyl surface (left), protonated decanamine molecules adsorbed to the siloxane surface (center) and protonated decanamine molecules closest to the siloxane surface, at least 0.5 nm from surface (right).

4   Conclusions

In this article, the authors have been able to describe the interaction between a range of organic molecules; including non-polar, polar, and ionic molecules, with the hydrated siloxane and hydroxyl mineral surfaces of kaolinite using molecular dynamic simulations. To the authors knowledge, this is the first time that such a systematic study has been carried out with a large amount of organic molecules on kaolinite.

The results present, in the first instance, the formation of clusters and micelle-like films

upon the siloxane surface for decane, decanoic acid and decanamine. Upon altering the pH of the system, and thus the charge of the organic molecules, drastic changes occur between the clay-organic interactions. As ionic interactions for charged organics overwhelm the weaker hydrogen bonding network between water and clay,[17] the affinity between organic molecules and hydroxyl surfaces can be drastically altered. The current work suggests that the charge of the organic molecule, and thus the pH of the system, has a particular relevance to alter the behaviour of the clay-organic interactions, with large implications for a wide range of applications, from surfactant treatments to enhanced oil recovery.

Additionally, the work presents how charge balancing ions play an important role in the interactions between organic matter and clay minerals. The simulation results present that both siloxane and hydroxyl surfaces will adsorb sodium ions, whilst chloride ions are selectively adsorbed to the hydroxyl surface. This unusual property warrants further examination, and is currently under investigation from the current authors. Anion bridging has also been observed between kaolinite and positively charged organics, a phenomenon not typically associated with clay minerals.

The work presents the important role that molecular dynamic simulations can play in elucidating the fundamental interactions between molecules at an atomic resolution. It shows the marked variety of properties that clay minerals possess, and that kaolinite exhibits a far richer range of chemistry compared to the typically examined 2:1 clay minerals. Further work on this topic will address the role of salt composition and concentration within the nanopore, and the function this plays upon the clay-organic interactions.

5   Acknowledgements

computing services. The authors also thank Rikan Kareem and Pablo Cubillas for the ESEM and AFM images respectively used in Figure 1.[12]

References

(1) Brady, P. V. *The Physics and Chemistry of Mineral Surfaces*; CRC Press: Boca Raton, FL, 1996.

(2) Vaughan, D.; Pattrick, R.; Mineralogical Society (Great Britain), *Mineral Surfaces (The Mineralogical Society Series)*; Chapman & Hall: New York, 1995; Vol. 5.

(3) Brown Jr, G. E. How Minerals React with Water. *Science* **2001**, *294*, 67–69.

(4) Bantignies, J.-L.; Moulin, C. C. D.; Dexpert, H. Wettability Contrasts in Kaolinite and Illite Clays: Characterization by Infrared and X-ray Absorption Spectroscopies. *Clays Clay Miner.* **1997**, *45*, 184–193.

(5) Wilson, M. J.; Wilson, L.; Patey, I. The Influence of Individual Clay Minerals on Formation Damage of Reservoir Sandstones: A Critical Review with some New Insights. *Clay Miner.* **2014**, *49*, 147–164.

(6) Greathouse, J. A.; Johnson, K. L.; Greenwell, H. C. Interaction of Natural Organic Matter with Layered Minerals: Recent Developments in Computational Methods at the Nanoscale. *Minerals* **2014**, *4*, 519–540.

(7) Suter, J. L.; Anderson, R. L.; Greenwell, H. C.; Coveney, P. V. Recent Advances in Large-Scale Atomistic and Coarse-Grained Molecular Dynamics Simulation of Clay Minerals. *J. Mater. Chem.* **2009**, *19*, 2482–2493.

(8) Greenwell, H. C.; Jones, W.; Coveney, P. V.; Stackhouse, S. On the Application of Computer Simulation Techniques to Anionic and Cationic Clays: A Materials Chemistry Perspective. *J. Mater. Chem.* **2006**, *16*, 708–723.

(9) Sposito, G.; Skipper, N. T.; Sutton, R.; Park, S.-h.; Soper, A. K.; Greathouse, J. A. Surface Geochemistry of the Clay Minerals. *Proc. Natl. Acad. Sci. U. S. A.* **1999**, *96*, 3358–3364.

(10) Wilson, M. J. The Origin and Formation of Clay Minerals in Soils: Past, Present and Future Perspectives. *Clay Miner.* **1999**, *34*, 7–25.

(11) Worden, R. H.; Morad, S. *Clay Mineral Cements in Sandstones (Special Publication 34 of the IAS)*; Wiley-Blackwell: Malden, MA, 2003.

(12) Cubillas, P.; Kareem, R. SEM and AFM Images of Kaolinite Clay Minerals. Unpublished Work.

(13) Brady, P. V.; Cygan, R. T.; Nagy, K. L. Molecular Controls on Kaolinite Surface Charge. *J. Colloid Interface Sci.* **1996**, *183*, 356–364.

(14) Schroth, B. K.; Sposito, G. Surface Charge Properties of Kaolinite. *Clays Clay Miner.* **1997**, *45*, 85–91.

(15) Tombácz, E.; Szekeres, M. Surface Charge Heterogeneity of Kaolinite in Aqueous Suspension in Comparison with Montmorillonite. *Appl. Clay Sci.* **2006**, *34*, 105–124.

(16) Sposito, G. *The Chemistry of Soils*; Oxford University Press: New York, 2008.

(17) Geatches, D. L.; Jacquet, A.; Clark, S. J.; Greenwell, H. C. Monomer Adsorption on Kaolinite: Modeling the Essential Ingredients. *J. Phys. Chem. C* **2012**, *116*, 22365–22374.

(18) Lee, S. G.; Choi, J. I.; Koh, W.; Jang, S. S. Adsorption of β-d-Glucose and Cellobiose on Kaolinite Surfaces: Density Functional Theory (DFT) Approach. *Appl. Clay Sci.* **2013**, *71*, 73–81.

(19) Johnson, E. R.; Otero-de-la Roza, A. Adsorption of Organic Molecules on Kaolinite from the Exchange-Hole Dipole Moment Dispersion Model. *J. Chem. Theory Comput.* **2012**, *8*, 5124–5131.

(20) Greathouse, J. A.; Geatches, D. L.; Pike, D. Q.; Greenwell, H. C.; Johnston, C. T.; Wilcox, J.; Cygan, R. T. Methylene Blue Adsorption on the Basal Surfaces of Kaolinite: Structure and Thermodynamics from Quantum and Classical Molecular Simulation. *Clays Clay Miner.* **2015**, *63*, 185–198.

(21) Underwood, T.; Erastova, V.; Cubillas, P.; Greenwell, H. C. Molecular Dynamic Simulations of Montmorillonite-Organic Interactions under Varying Salinity: An Insight into Enhanced Oil Recovery. *J. Phys. Chem. C* **2015**, *119*, 7282–7294.

(22) Downs, R. T.; Hall-Wallace, M. The American Mineralogist Crystal Structure Database. *Am. Mineral.* **2003**, *88*, 247–250.

(23) Bish, D. L. Rietveld Refinement of the Kaolinite Structure at 1.5 K. *Clays Clay Miner.* **1993**, *41*, 738–744.

(24) Martínez, L.; Andrade, R.; Birgin, E. G.; Martínez, J. M. PACKMOL: a Package for Building Initial Configurations for Molecular Dynamics simulations. *J. Comput. Chem.* **2009**, *30*, 2157–2164.

(25) Barratt, M. Quantitative Structure-Activity Relationships (QSARs) for Skin Corrosivity of Organic Acids, Bases and Phenols: Principal Components and Neural Network Analysis of Extended Datasets. *Toxicol. In Vitro* **1996**, *10*, 85–94.

(26) Perrin, D. D. *Ionisation Constants of Inorganic Acids and Bases in Aqueous Solution*; Pergamon Press: Exeter, UK, 1984.

(27) Hanwell, M. D.; Curtis, D. E.; Lonie, D. C.; Vandermeersch, T.; Zurek, E.; Hutchi-

son, G. R. Avogadro: An Advanced Semantic Chemical Editor, Visualization, and Analysis Platform. *J. Cheminf.* **2012**, *4*, 17.

(28) Yin, X.; Gupta, V.; Du, H.; Wang, X.; Miller, J. D. Surface Charge and Wetting Characteristics of Layered Silicate Minerals. *Adv. Colloid Interface Sci.* **2012**, *179*, 43–50.

(29) Jiang, T.; Hirasaki, G. J.; Miller, C. A. Characterization of Kaolinite ζ Potential for Interpretation of Wettability Alteration in Diluted Bitumen Emulsion Separation. *Energy Fuels* **2010**, *24*, 2350–2360.

(30) Cygan, R. T.; Liang, J.-J.; Kalinichev, A. G. Molecular Models of Hydroxide, Oxyhydroxide, and Clay Phases and the Development of a General Force Field. *J. Phys. Chem. B* **2004**, *108*, 1255–1266.

(31) Vanommeslaeghe, K.; Hatcher, E.; Acharya, C.; Kundu, S.; Zhong, S.; Shim, J.; Darian, E.; Guvench, O.; Lopes, P.; Vorobyov, I. et al. CHARMM General Force Field: A Force Field for Drug-like Molecules Compatible with the CHARMM All-Atom Additive Biological Force Fields. *J. Comput. Chem.* **2010**, *31*, 671–690.

(32) Bjelkmar, P.; Larsson, P.; Cuendet, M. A.; Hess, B.; Lindahl, E. Implementation of the CHARMM Force Field in GROMACS: Analysis of Protein Stability Effects from Correction Maps, Virtual Interaction Sites, and Water Models. *J. Chem. Theory Comput.* **2010**, *6*, 459–466.

(33) Pastor, R. W.; MacKerell Jr, A. D. Development of the CHARMM Force Field for Lipids. *J. Phys. Chem. Lett.* **2011**, *2*, 1526–1532.

(34) Wright, L. B.; Walsh, T. R. First-Principles Molecular Dynamics Simulations of NH_4^+ and CH_3COO^- Adsorption at the Aqueous Quartz Interface. *J. Chem. Phys.* **2012**, *137*, 224702.

(35) Skelton, A.; Fenter, P.; Kubicki, J. D.; Wesolowski, D. J.; Cummings, P. T. Simulations of the Quartz(1011)/Water Interface: A Comparison of Classical Force Fields, Ab Initio Molecular Dynamics, and X-ray Reflectivity Experiments. *J. Phys. Chem. C* **2011**, *115*, 2076–2088.

(36) Hess, B.; Kutzner, C.; van der Spoel, D.; Lindahl, E. GROMACS 4: Algorithms for Highly Efficient, Load-Balanced, and Scalable Molecular Simulation. *J. Chem. Theory Comput.* **2008**, *4*, 435–447.

(37) Pronk, S.; Páll, S.; Schulz, R.; Larsson, P.; Bjelkmar, P.; Apostolov, R.; Shirts, M. R.; Smith, J. C.; Kasson, P. M.; van der Spoel, D. et al. GROMACS 4.5: a High-Throughput and Highly Parallel Open Source Molecular Simulation Toolkit. *Bioinformatics* **2013**, *29*, 845–854.

(38) Humphrey, W.; Dalke, A.; Schulten, K. VMD: Visual Molecular Dynamics. *J. Mol. Graphics* **1996**, *14*, 33–38.

(39) Michaud-Agrawal, N.; Denning, E. J.; Woolf, T. B.; Beckstein, O. MDAnalysis: A Toolkit for the Analysis of Molecular Dynamics Simulations. *J. Comput. Chem.* **2011**, *32*, 2319–2327.

(40) Swadling, J. B.; Coveney, P. V.; Greenwell, H. C. Clay Minerals Mediate Folding and Regioselective Interactions of RNA: A Large-Scale Atomistic Simulation Study. *J. Am. Chem. Soc.* **2010**, *132*, 13750–13764, PMID: 20843023.

(41) Swadling, J. B.; Suter, J. L.; Greenwell, H. C.; Coveney, P. V. Influence of Surface Chemistry and Charge on Mineral-RNA Interactions. *Langmuir* **2013**, *29*, 1573–1583.

(42) Thyveetil, M.-A.; Coveney, P. V.; Suter, J. L.; Greenwell, H. C. Emergence of Undulations and Determination of Materials Properties in Large-Scale Molecular Dynamics Simulation of Layered Double Hydroxides. *Chem. Mater.* **2007**, *19*, 5510–5523.

(43) Thyveetil, M.-A.; Coveney, P. V.; Greenwell, H. C.; Suter, J. L. Role of Host Layer Flexibility in DNA Guest Intercalation Revealed by Computer Simulation of Layered Nanomaterials. *J. Am. Chem. Soc.* **2008**, *130*, 12485–12495.

(44) Underwood, T.; Erastova, V.; Greenwell, H. C. Ion Adsorption at Smectite Clay Mineral Surfaces: A Hofmeister Series for Hydrated Smectite Mineral. *Clays Clay Miner.* **2016**, Submitted.

(45) Hu, X. L.; Michaelides, A. Water on the Hydroxylated (001) Surface of Kaolinite: From Monomer Adsorption to a Flat 2D Wetting Layer. *Surf. Sci.* **2008**, *602*, 960–974.

(46) Hu, X. L.; Michaelides, A. Ice Formation on Kaolinite: Lattice Match or Amphoterism? *Surf. Sci.* **2007**, *601*, 5378–5381.

Graphical TOC Entry